euspen's 16th International Conference & Exhibition, Nottingham, UK, May 2016
www.euspen.eu

One step fabrication and characterisation of stainless steel superhydrophobic surfaces using laser ablation

Yanling Tian[1], Xianping Liu[1], Susan Burrows[2]

[1]School of Engineering, University of Warwick, Coventry CV4 7AL, UK
[2]Department of Physics, University of Warwick, Coventry CV4 7AL, UK
Email: y.tian.1@warwick.ac.uk

Abstract
Superhydrophobicity of several natural plants and animals provides the excellent mechanical and physical properties. A number of research efforts have been directed to imitate and design the functional surfaces with superhydrophobicity. However, the durability of the metallic superhydrophobic surfaces is one of the main problems to block their applications. To overcome this problem, a one-step laser ablation based fabrication methodology for stainless steel superhydrophobic surfaces has been proposed. Through carefully optimizing the machining parameters, the superhydrophobic surfaces on stainless steel can be obtained without further surface coating treatment, which provides a cost-effective and high efficiency fabrication methodology. Since the top layer is directly formed from the bulk material, the long-term durability and resistance for mechanical wear and corrosion can be maintained. In addition, it is cheap for there is no further surface coating required. In order to investigate the inherent mechanism of wettability change on stainless steel, a number of extensive surface metrology and characterisation has been conducted. The relationships between the wettability and the surface topography have been extensively explored. It is noted that the surface topography can be modified by the laser ablation, and the contact angle can be improved or reduced due to the increase of the contact area. The wettability change is dependent on the laser fluence on the surface. Smaller laser fluence can improve the contact angle to some extent, and the larger one will make the surface superhydrophilic at the beginning. However, the superhydrophilic surfaces can change into superhydrophobic surfaces after several days. Through the experiments, it is noted that the reason for this wettability transition is not due to surface topography change but the chemistry alternation of the top layer. The developed fabrication and characterisation methodologies put one step forward for practical application of the metallic superhydrophobic surfaces in the industrial and academic sectors.

Keywords : Superhydrophobicity, stainless steel, laser ablation, surface metrology and characterisation

1. Introduction

The excellent self-cleaning/anti-adhesion performance of the nature plants and animals has attracted extensive research efforts for many decades [1, 2]. A number of biomimetic and engineering methodologies have been developed to generate the self-cleaning surfaces. It has been demonstrated that super-hydrophobic surfaces can only be achieved by combining hydrophobicity with appropriate surface texture [3, 4]. A number of methods have been developed to achieve the superhydrophobic surfaces. However, the available fabrication methodologies for silicon, polymer and metal surfaces make them fragile and weak for mechanical contacts including scratching, corrosion, and wear.

This paper presents the one step fabrication of the superhydrophobic surfaces on stainless steel surface using nanosecond laser ablation technique. Since the top layer of the metallic superhydrophobic surface is directly formed from the bulk material, the long-term durability and resistance for mechanical wear and corrosion of the superhydrophobicity can be maintained. The relationships between the wettability and the surface topography have been explored. The wettability change is dependent on the laser fluence on the surface.

2. Experimental method

Machine tool: A commercial nanosecond laser machine (Oxford E-Series, UK) is used to fabricate the stainless steel surfaces. The diode pumped solid state (DPSS) Nd:YAG laser is utilized to conduct the machining. The parameters of the laser are as follows: the maximum output power is 6 W, the wavelength of the laser is 355 nm, the pulse duration is 34 ns, and the repetition rate ranges from 5 kHz to 20 kHz. The polarized Gaussian-profile laser beam was focused to a spot with diameter of 30 µm. The ablation process was performed in the atmospheric environment under normal incidence of the laser beam. The laser scanning was conducted line by line with the line space of 30 µm.

Workpiece material: The stainless steel (304) is utilized to conduct the hydrophobic surface fabrication. The workpiece is cut from as delivered rolled strip using the WEDM (Wire Electrical Discharge Machining) technique. The samples are cleaned using the compressed air, and the ultrasonic bath with the deionized water, alcohol and acetone.

3. Results and discussions

In the current experiment testing, the ablation power of the laser is chosen as 0.5%, 5%, and 20% of the maximum value, i.e.0.03 W, 0.3 W and 1.2 W. The repetition rate is set as 10 kHz, and the scanning speed is 5 mm/s for raster scanning. The laser fluences are equal to 0.424 J/cm2, 4.24 J/cm2 and 16.98 J/cm2 (for 0.5%, 5% and 20% of maximum power, respectively) in the experimental testing. These values are higher than the ablation threshold fluence of stainless steel [5]. When the fluence is less than 1 J/cm2, the laser ablation process is defined as the gentle ablation, and the fluences larger than 1 J/cm2, the ablation is considered as the strong ablation.

Fig.1 shows the contact angle measurement of the stainless steel with and without laser ablation treatments. It is noted that the untreated/original surface of the stainless steel has small contact angle CA=78°. However, the contact angle can be improved and could reach up to more than 154° after laser ablation. However, it must be pointed out that there exits the

wettability transformation on the ablated surface. The evolution of the wettability is illustrated in Fig.2. It can be seen that the ablated surface shows the superhydrophilicity at the beginning of the evaluation, and the contact angle increases with the increasing time of the samples exposed in air. Under the strong ablation condition, the water droplet spreads on the ablated surface at the beginning, i.e. the contact angle equals to zero. With the time increasing, the contact angle dramatically increases and reaches up to 150˚. It is also noted that the wettability transform firstly occurs at the lower fluence, and then happens at the higher fluence. On the contrary, the wettability of stainless steel surface has little changes under the gentle ablation. It can be seen that there is slight increase of the contact angle, from 96.5˚ to 100.2˚, and no contact angle decrease.

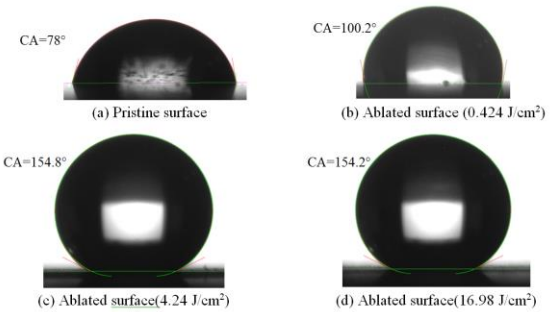

Figure 1. Contact angle of the ablated stainless steel.

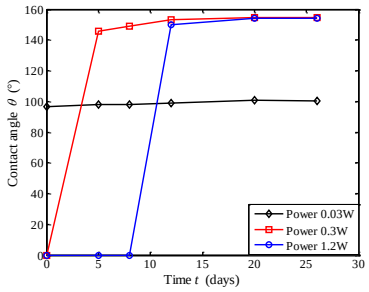

Figure 2. Time dependent contact angle of ablated surfaces.

The SEM images have been taken using the Philips XL-30 ESEM. The multi-scale topography of ablated surfaces is shown in Fig.4. The pristine surface is measured and shown in Fig. 4(a). It can be seen that the top surface of the pristine material undergoes the plastic deformation due to the rolling process to prepare the stainless steel strip. The pristine surface has a number of cavities with the cracks. After the stainless steel surface is ablated, the periodical line pattern is formed along with the laser scanning direction. In the case of the gentle ablation (laser power 0.03 W), the line pattern is form by the recast strips in the process of melt and resolidation. It is noted that the microholes are formed at the edges the recast strips. When the laser power increases up to 0.3 W, the grooves with high aspect ratio are formed on the ablated surface. The walls between the neighbour grooves are formed by the recast layers, and there are a number of ripple in the horizontal and vertical directions on the sidewalls of the grooves. When the laser power reaches up to 1.2 W, the bumps are formed and separated with grooves in the scanning direction and the orthogonal direction. The diameter of the bumps is approximately 25 μm. The bumps are covered by the fine spherical structures and micro holes.

EDX analysis has been conducted to measure the elemental composition on the top surface. The pristine sample mainly contains the elements including Fe, Cr, Ni, Si, and C. It can be

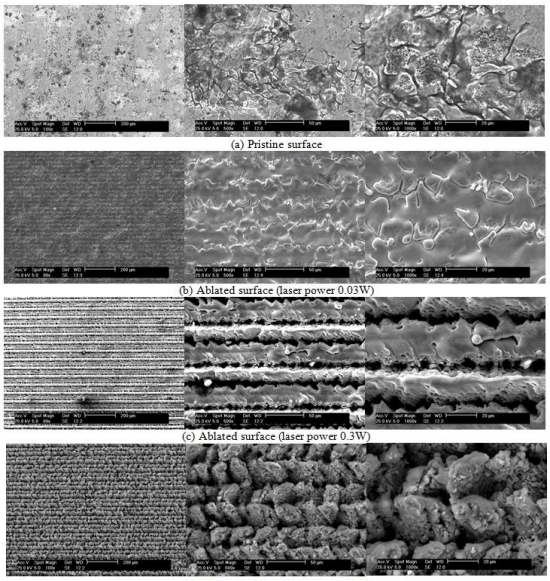

Figure 3. SEM images of the machined stainless steel.

seen that the element O has a significant increase especially for the strong ablations. The change details of the elements O and C are shown in Table 1. . It is noted that the atomic percentages of C and O have increased from 28.68% and 9.40% (pristine surface) to 43.75% and 24.85% (laser power 0.3 W), 42.52% and 25.65% (laser power 1.2W), respectively. The increase of the element O will increase the hydrophilicity of the surface, since the metal oxidise can increase the polarity of the top surface. However, this cannot explain the wettability transformation observed in the experimental testing. Thus, the increase of the element C must be the main reason for the transformation

Table 1. Element analysis of the stainless steel surfaces.

	Element Atomic Percentage (at%)			
Laser power	Pristine	0.03 W	0.3 W	1.2 W
C	28.68	31.46	43.75	42.52
O	9.40	13.28	24.85	25.65
Fe	35.07	38.78	20.72	21.12

4. Conclusions

Laser ablation technique is utilized to change the wettability of the stainless steel, which can provide long durability, high efficiency and low cost fabrication method. The patterned surfaces including a number of hierarchic micro-structures and microholes increase the contact area between the water droplet and the stainless steel surfaces. In addition, the chemistry and wettability of the ablated surfaces has been changed into hydrophobic by appearance of new functional groups including methyl group -CH3 and graphitic C.

References

[1] Zhang Y., Chen Y., Shi L., Li J., and Guo Z. 2012, J. Mater. Chem., **22** 799-815.

[2] Zhang L., Zhao N., and Xu J. 2014, J. Adhes. Sci. Technol., **28** 769-790.

[3] Liu Y., Liu J., Li S., Han Z., Yu S., and Ren L. 2014, J. Mater. Sci., **49** 1624-1629.

[4] Choi H., Choo S., Shin J., Kim K., and Lee H. 2013, J. Physic. Chem., **117** 24354-24359.

[5] Mannion P., Magee J., Coyne E., O'Connor G., and Glynn T. 2004, Appl. Surf. Sci., **233** 275-287.